ELSEVIER

Computers & Geosciences 33 (2007) 808–820

COMPUTERS & GEOSCIENCES

www.elsevier.com/locate/cageo

Numerical modelling of fault activities ☆

Hilmar Bungum*

NORSAR/ICG, P.O. Box 53, N-2027 Kjeller, Norway

Received 3 February 2006; received in revised form 16 October 2006; accepted 25 October 2006

Abstract

There is a fundamental connection between crustal strain (deformation) rates and seismic activity. To this end two FORTRAN utility programs have been developed, aimed at estimating the seismicity on a fault in cases when this cannot be done directly, or as a comparison with observed data. The first program (''moment_slip'') is one in which seismicity is derived from the rate of seismic slip, based on published models for the connection between slip rates and seismic activity. The size of the fault is essential here, constraining the maximum magnitude. The slope of the frequency–magnitude distribution and its functional form are other important controlling parameters. The key physical concept in this connection is seismic moment release, which is related to magnitude through specified moment–magnitude relationships. For cases when slip rates are not available a second program (''moment_rate'') has been developed, aimed at computing the recurrence rate from an estimate of the moment release, inferred for example from historical and/or recent seismicity in the region in which the fault is located. A number of sensitivity tests demonstrate the relative importance of the different assumptions and parameters.

Keywords: Seismicity; Seismic moment; Fault area; Slip rate; Maximum magnitude

1. Introduction

Seismic hazard estimations are essentially predictions of which ground motions one should expect from future earthquakes. Such assessments started with deterministic methods, asking which kind of earthquakes a given (building) site possibly could be exposed to, where they could be located and with which magnitude. This is essentially a scenario-based approach. Probabilistic methods on the other hand are essentially statistically based assessments (Cornell, 1968; McGuire, 1976, 1978) in which a range of seismic sources are considered, each with their own occurrence probabilities and influence on the site: dependent on the distance and frequency of motion. The key product here is the so-called hazard curve which usually provides expected ground motions versus yearly probabilities (or return periods), which can be provided with confidence intervals if a logic-tree (or Monte Carlo) approach is applied (Kulkarni et al., 1984; Coppersmith and Youngs, 1986; Bommer et al., 2005).

Seismic hazard analysis methods have a wide range of applications, from broadly based zonations aimed essentially only at describing and delineating the seismicity, to site-specific analyses aimed specifically at design. Within both fields the analyses

☆ Code available from server at http://www.iamg.org/CGEditor/index.htm?

*Tel.: +47 63805934; fax: +47 63818719.
E-mail address: hilmar.bungum@norsar.no.

0098-3004/$ - see front matter © 2007 Elsevier Ltd. All rights reserved.
doi:10.1016/j.cageo.2006.10.011

range from relatively cursory to highly detailed, with the level of detail for design purposes being dependent on the sensitivity of the installation. The key predictive element in any seismic hazard analysis, both probabilistic and deterministic, is the source model which specifies the expected spatio-temporal distribution of earthquakes within the range of distances which could potentially influence the site. For deterministic methods the source model is usually a specific fault, while for probabilistic methods it is often some combination of area sources (of homogeneous seismicity) and specific faults.

The dynamic processes behind earthquakes are those that are expressed in terms of crustal deformation or strain rates, which range from about $10^{-6}\,\mathrm{yr}^{-1}$ in the tectonically most active regions and possibly as low as $10^{-13}\,\mathrm{yr}^{-1}$ in more stable continental interiors (Bungum et al., 2005; Calais et al., 2006). These are average numbers, however, and what matters the most in terms of crustal deformation at a specific site is the slip rate (often in units of mm/yr) on the potentially active faults. Normally, the fault activity is estimated directly by monitoring the seismicity over some time, extrapolating this into the future from statistical occurrence models in combination with an independent assessment of maximum magnitude. This is not always possible, however, especially if the activity is low but still potentially important, and it is for such cases that the algorithms in this paper have been developed.

Various strategies may for such cases be chosen for the assessment of earthquake activities on faults, depending on which information is available for characterizing the fault movement, the age of the last movement (which is instrumental for calling the fault "active" or not), the size of the fault, its partitioning, etc. In cases where slip rates on faults are available directly, algorithms based on such estimates are considered to represent the most viable alternative provided that the derived activity is always assessed in terms of the equivalent moment release.

When slip rates are not available the earthquake activity on a fault has to be assessed by other means, usually by assigning to the fault a certain proportion of the seismic activity which is assessed for the region containing the fault. In this case also it is important to consider the moment rate budget, rather than the number of events, or the magnitude–frequency distribution. Since the contribution to seismic moment increases strongly with magnitude, the maximum magnitude becomes very critical in this respect.

For the purpose of this study we have developed two different utility programs which may be useful for quantifying earthquake activity on faults in both of the above cases, as documented in the following sections. We include also sensitivity tests that help to determine the relative importance of the various parameters.

2. Fault activity from slip rates

In calculating seismic hazard, the seismicity which is assigned to an individual fault is, as for the area sources, usually assumed to follow the classical cumulative Gutenberg–Richter relationship:

$$\log N = a + bM, \tag{1}$$

where N is the number of earthquakes equal to or above magnitude M, and a and b are constants. Here, a determines the absolute activity level while b determines the slope of the curve (usually around 1.0), or the ratio between smaller and larger earthquakes. The distribution is limited at the upper end by the maximum magnitude $M_{\max}$ where a sharp cutoff may be assumed, and at the lower end by a lower bound or reference magnitude (usually around magnitude 4–5) which is the starting point for the seismic hazard integration. The lower cutoff is essentially determined from engineering considerations, separating between events that are of engineering importance or not. Formally, the cumulative occurrence relationship in this case can be expressed as (Chinnery and North, 1975):

$$N(M) = 10^{(a_1 - bM)} H(M_{\max} - M), \tag{2}$$

where $H(\cdot)$ is the Heaviside step function. This form, shown in Fig. 1, has been commonly used in probabilistic seismic hazard analyses. The form of truncation means that this model is particularly enriched in large magnitude earthquakes.

Normally, b-values for area sources are, as already noted, around 1.0, implying a factor of 10 reduction in the number of events per magnitude unit. The b-value assigned to recurrence for faults is often (but not necessarily) lower, however, reflecting the narrower probability density function for magnitudes relating to just one particular fault.

Physically, a reason for a lower b-value for faults may be tied to the concept of "characteristic earthquakes", which is supported theoretically as

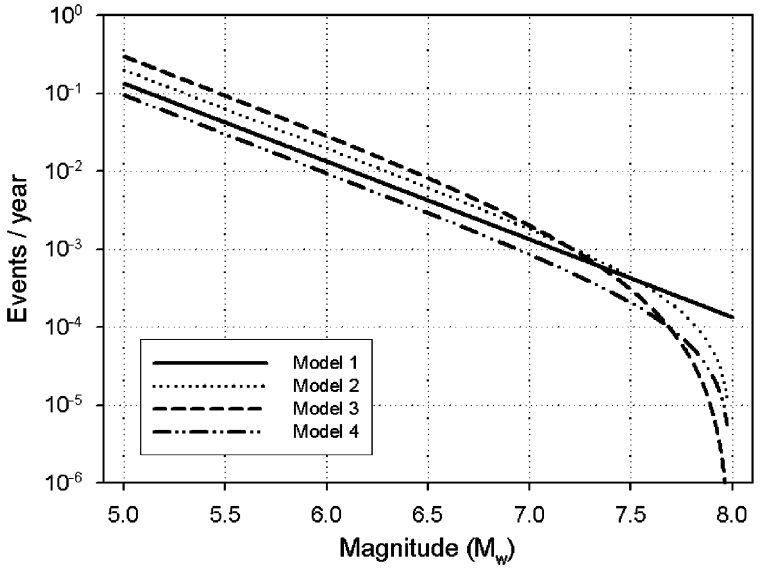

Fig. 1. Cumulative recurrence relationships for Models 1–3 (Anderson and Luco, 1983) and Model 4 (Youngs and Coppersmith, 1985) used in this paper, based on a fault that allows for a maximum magnitude of 8.0 (fault length 120 km and a length/width ratio of 2), a slip/length ratio of 10^{-5}, a shear modulus of 30 GPa, a slip rate of 1 mm/yr and a *b*-value of 1.0.

well as by observational data (Swan et al., 1980; Papageorgiou and Aki, 1983), but also challenged (Grant, 1996; Bakun et al., 2005). This concept involves the assumption that most of the energy released (or the slip) on a fault is accounted for through earthquakes which are generally of about the same magnitude. The low *b*-values that this would imply are not necessarily in conflict with larger values regionally (for area sources) where the contribution from a variety of faults, large and small, is accounted for.

The estimation of activity rates (N-values) involves also the seismic moment, M_0, the rigidity, or shear modulus, μ, the total average displacement (or slip) across the fault, D, and the rupture area, $A = LW$, where L is fault length and W is fault width. These parameters come directly into play in the well-known physical definition of seismic moment for a particular earthquake (e.g., Aki et al., 2002):

$$M_0 = \mu DA. \tag{3}$$

Assuming conservatively that all of the fault slip occurs seismically (i.e., a coupling coefficient of 1.0), the total moment release rate (such as moment per year) $\dot{M}_0{}^T$ is related to the slip rate (annual movement) of the fault as follows (Brune, 1968):

$$\dot{M}_0{}^T = \mu SA, \tag{4}$$

where S is the annual slip (i.e., the slip rate), ignoring possible aseismic creep (Anderson et al., 1993). It is recognized that $\dot{M}_0{}^T$ should be averaged over several cycles of large earthquakes for this relation to be valid (Anderson, 1979; see also Molnar, 1979).

Based on Eqs. (2)–(4), Anderson and Luco (1983) deduced the following relationship for the determination of the number of earthquakes N above the lower bound magnitude (normally around 4–5) on a fault:

$$N_1(M) = \left(\frac{\bar{d} - \bar{b}}{\bar{d}}\right)\left(\frac{S}{\beta}\right) e^{\bar{b}(M_{\max} - M)}\, e^{-((\bar{d}/2)M_{\max})}, \tag{5}$$

where $\bar{b} = b(\ln(10))$, $\bar{d} = d(\ln(10))$, $\beta = \sqrt{(\alpha M_0(0))/(\mu W)}$, $\alpha = D/L$, and $M_0(0)$ is the seismic moment for $M_S = 0$.

The parameter d is the magnitude scaling coefficient in the well-known log-linear relation between moment and magnitude, of the form $\log M_0 = c - dM$ (e.g., Kanamori and Anderson, 1975).

Anderson and Luco (1983) also developed similar relationships for two other recurrence models in addition to Eq. (5), firstly the incremental relation

$$n_2(M) = 10^{(a_2 - bM)} H(M_{\max} - M), \tag{6}$$

as advocated by Båth (1978), Anderson (1979) and Berril and Davis (1980). In its cumulative version,

this occurrence relation has a more smooth (rounded) transition towards $N(M_{\max}) = 0$. This is occurrence relation 2 in Anderson and Luco (1983), or Model 2 in the present paper, tied to the following relation for N:

$$N_2(M) = \left(\frac{\bar{d} - \bar{b}}{\bar{b}}\right)\left(\frac{S}{\beta}\right)\left[e^{\bar{b}(M_{\max} - M)} - 1\right]e^{-((\bar{d}/2)M_{\max})}. \quad (7)$$

Occurrence relation 3 in Anderson and Luco (1983), or Model 3 in the present paper, is one proposed by Main and Burton (1981):

$$n_3(M) = (10^{(a_3 - bM)} - 10^{(a_3 - bM_{\max})})H(M_{\max} - M), \quad (8)$$

which has an even gentler transition towards $N(M_{\max}) = 0$. The corresponding N-relation in this case reads

$$N_3(M) = \frac{\bar{d}(\bar{d} - \bar{b})}{\bar{b}}\left(\frac{S}{\beta}\right)\left\{\frac{1}{\bar{b}}\left[e^{\bar{b}(M_{\max} - M)} - 1\right] - (M_{\max} - M)\right\}e^{-((\bar{d}/2)M_{\max})}. \quad (9)$$

For all of these three Anderson and Luco (1983) models (Eqs. (5), (7) and (9)), the annual number of events N above a given magnitude M is the inverse of the return time T in years, for the same magnitude, i.e., $T = 1/N$.

In addition to these three models, we have also included in this paper a Model 4, as developed by Youngs and Coppersmith (1985), and which is supposed to be quite close to Model 2:

$$N_4(m^0) = \frac{\mu A_f S(d - b)[1 - e^{-\beta(m^u - m^0)}]}{bM_0^u e^{-\beta(m^u - m^0)}}, \quad (10)$$

where m^0 is some arbitrary reference magnitude, $m = b\ln(10)$, $A_f = LW$ is fault area and m^u is an upper bound magnitude. Models 1–4 presented here are derived from Equations I.10, II.9 and III.9 in Anderson and Luco (1983) and from Equation 11 in Youngs and Coppersmith (1985), respectively, and the cumulative recurrence rates from the models are also shown in Fig. 1. For more details about the models and the assumptions they are derived from we refer to these papers and to Anderson et al. (1993).

The main purpose of the present paper is to apply and test these four models, and to this end we have developed a FORTRAN utility program "moment_slip" where all of the models are included, and with a parameterization as shown in Table 1. Line 3 in that table refers to the fact that the program loops over a range of fault lengths, essentially with individual runs for each fault length (or fault size). The program could of course be run only with just one fault length, but experience shows that the scaling properties often are interesting here, not least in relation to the magnitude potentials (maximum magnitude). In addition, the fault length is often a poorly constrained parameter, and in this sense the program will demonstrate clearly what the consequences of different interpretations will be.

For a long fault, and in particular a fault system, some segmentation is usually needed when evaluating the potential seismicity, or the recurrence characteristics. An earthquake segment refers normally to those parts of a fault zone that have ruptured during individual earthquakes, where the segments are separated by some kind of discontinuity that may be either geology-based (geometric, structural) or behavioural (slip rates, seismicity, displacements, etc.) (Yeats et al., 1997). The length of the segment is an important constraining parameter for the maximum magnitude.

In returning to Table 1 it should be noted here that when a magnitude scale other than moment magnitude M_W is used, relations to M_W are established either through a user-defined moment–magnitude relation (line 7) combined with the Hanks and Kanamori (1979) M_0–M_W relation, or through a standard (global) M_W–M_S relation when M_S is used (Okal and Romanowicz, 1993). Using this utility program, a number of sensitivity tests have been conducted and documented in the following.

One of the models that are needed in these calculations is the relation between magnitude and fault area (line 8 in Table 1), where the numbers in the table refer to the classical Wyss (1979) relation. This relation is shown in Fig. 2 together with that of Nuttli (1983), developed for intraplate conditions, and those of Wells and Coppersmith (1994), for the three different modes of faulting. Anderson et al. (1996) have also developed a relation that is quite close to that of Wells and Coppersmith (1994) but which also includes slip rate, and where a higher slip rate reduces the maximum magnitude. As for relations between moment and magnitude those connecting magnitude to fault area often vary regionally, and in particular so between plate margin and intraplate regions.

The differences between the four recurrence models documented above are shown in Fig. 3, together with the average and the standard devia-

Table 1
Input parameters used in the computer program "moment_slip", with examples of possible values

Line	Parameter	Example values		
1	Model type: 1–3: Anderson and Luco (1983); 4: Youngs and Coppersmith (1985); 5: average of 1–4.	5		
2	Fault slip rate (mm/yr)	1.0		
3	Fault length range: min, max and step length (km)	5.0	45.0	2.5
4	b-value in $\log(N) = a - b \cdot M$	1.0		
5	Reference magnitude for N-value calculation	4.0		
6	Magnitude type (1: M_W, 2: M_S, 3: user-defined)	1		
7	Moment–magnitude relation: $\log(M_0) = c + d \cdot M$	$c = 16.05$	$d = 1.5$	
8	Fault area to M_{max} relation: $\log(A) = a + b \cdot M_{max}$	$a = -4.15$	$b = 1.0$	
9	Fault slip to fault length ratio	10^{-4}		
10	Fault length to fault width factor (L/W)	2.0		
11	Shear modulus (GPa)	30		

The program loops over a range of fault lengths, or essentially fault areas since the length/width ratio is also given, and for each of these it computes the activity rates and corresponding return times, based on the other parameters specified in the table, for the model given in line 1. For model type 5 both the average (of the four base models) and the standard deviation are computed.

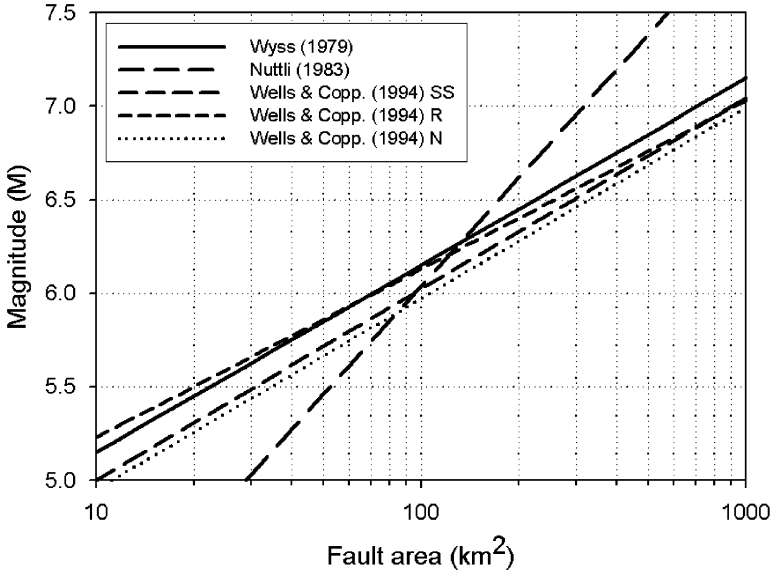

Fig. 2. Relation between fault area and moment magnitude using relations published by Wyss (1979), Nuttli (1983) and Wells and Coppersmith (1994), the latter for strike-slip (SS), reverse (R) and normal (N) faulting events. Note that the Nuttli (1983) relation is for intraplate conditions, explaining the difference in slope.

tion. The difference between the models is, as shown in Fig. 1 and also discussed by Anderson and Luco (1983) and Youngs and Coppersmith (1985), essentially the way in which the underlying occurrence relation behaves close to the upper bound magnitude. Model 1 is the most conservative one in this sense, assuming an abrupt cutoff and thereby allowing more moment release to occur close to the maximum magnitude, resulting in a higher activity rate. Even so, the scatter is only about a factor of 2 in activity rate, which is not more than what most experienced hazard analysts would assume for any activity rate uncertainty, and the differences between the models are small also when compared with the magnitude sensitivity, which is shown in Fig. 4. The sensitivity to fault length is log-linear only for some of the models in Fig. 3.

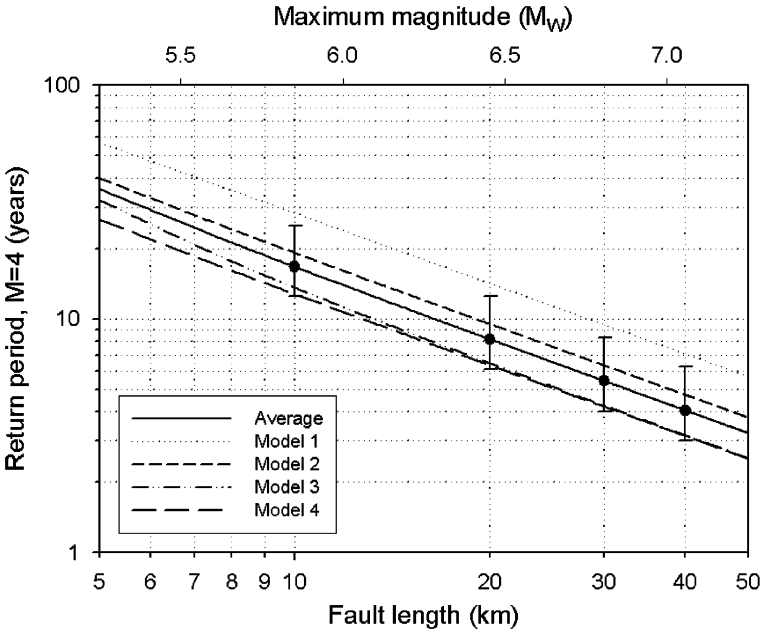

Fig. 3. Relation between return period for magnitude 4 earthquakes on a fault and fault length, for the four activity rate models and their average, with error bars for one standard deviation. The relations are based on a fault length twice the width, a slip rate of 1 mm/yr, a b-value of 1, a fault slip/length ratio of 10^{-4}, a rigidity of 30 GPa and a fault area versus maximum magnitude relation of $\log(A) = -4.15 + M_{\max}$. The x-axis is drawn both for fault length and maximum magnitude. The return period on the y-axis is the inverse of the activity rates, or the N-values. These parameters are used also in the subsequent figures.

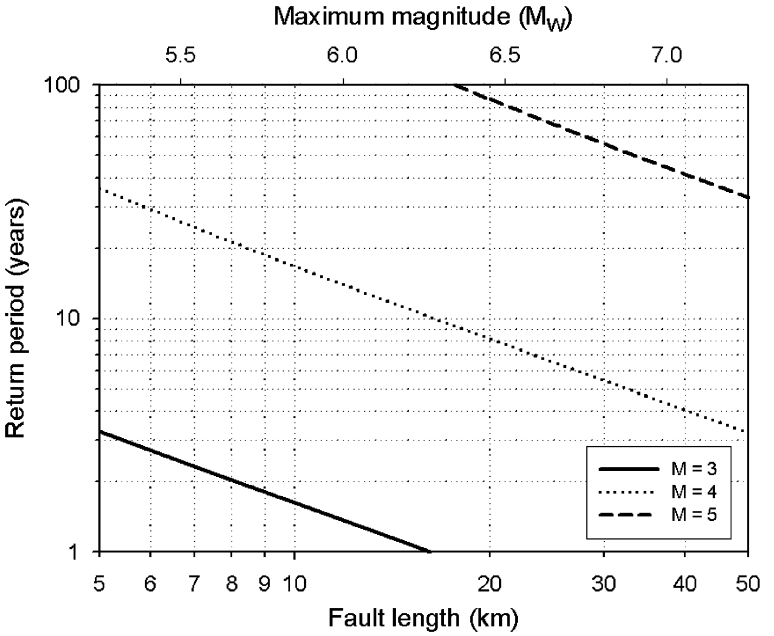

Fig. 4. Relation between return period for magnitude (M_W) 3, 4 and 5 earthquakes on a fault and fault length. Parameters otherwise are as for Fig. 3 (the solid line in Fig. 3 is identical to the line for $M = 4$ in Fig. 4).

The average of the four slip rate models is introduced in Fig. 4, showing the return period for threshold magnitude of 3, 4 and 5 as a function of fault length, assuming that the length is twice the width ($L = 2W$), for a case when the slip rate is 1 mm/yr. The return period here is simply the

inverse of the annual number of events. The earthquake frequency increases strongly (and the return period decreases) with fault length, given a constant slip rate. In these and the following calculations we have assumed the b-value to be 1, the magnitude fault area relation as in Table 1 (using Wyss, 1979), and the slip to fault length ratio to be 10^{-4} (e.g., Scholz, 2002). The rigidity (shear) modulus is here set to 30 GPa, which is a commonly used crustal average. For shallow faulting, however, the rigidity may decrease significantly (e.g., Bilek and Lay, 1999), leading to a proportionally increased displacement for the same seismic moment (Eq. (3)).

The sensitivity of the activity rate (again in terms of return period) with respect to slip rate is analysed in Fig. 5, where the parameters otherwise are defined as in Fig. 3. The sensitivity to slip rate is log-linear, which is easily seen also from Eqs. (5), (7) and (9). Please note that the return period (activity rate) scale in Fig. 5 covers five orders of magnitude, showing a strong sensitivity both to fault length and slip rate.

The ratio between fault slip and fault length, or the strain drop, is another important parameter where the sensitivity is shown in Fig. 6, in this case for fault lengths of 10 and 50 km. The two curves represent fixed values of fault length and thereby also M_{max}, and since the slip rate and seismic moment rate also are constant the change in earthquake frequency (or return period) is therefore related directly to the change in stress drop, being proportional to the strain drop. The range used there for this ratio covers the commonly reported range for this parameter, even though 10^{-3} may be on the high side. It could be noted here that intraplate conditions may imply higher strain drops and thereby also more moment release (see Eq. (3)), which is consistent with the difference in slope for the Nuttli (1983) relation in Fig. 2. Please note that the relations in Fig. 6 are not linear in log–log space.

The final sensitivity test from the "moment_slip" program is shown in Fig. 7, in this case with respect to the rigidity (shear) modulus. Eq. (3) shows that the rigidity also scales linearly with seismic moment, and for faulting other than in crystalline bedrock it may be unconservative to use the crustal average of 30 GPa (equivalent to 3×10^{11} dyn/cm^2) for this parameter. As is well known, the shear modulus, being the product of the density and the square of the shear velocity, may easily drop a factor of 10 even in fairly well-consolidated sediments, as compared with crystalline rocks. For a given seismic moment (or magnitude), Eq. (3) shows in this respect that a factor of 10 in reduced rigidity means a 10 times larger fault displacement. What is seen in Fig. 7 in this respect is that, as the rigidity increases, more moment will be released over a similar fault area, thereby reducing the return time between earthquakes of a given magnitude.

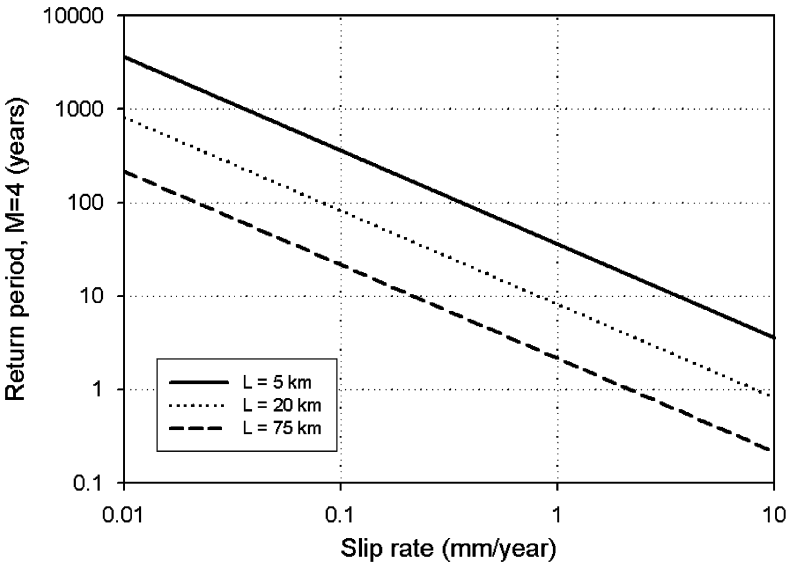

Fig. 5. Relation between return period for $M = 4$ earthquakes on a fault and slip rate, for fault lengths of 5, 20 and 75 km. Parameters otherwise are as for Fig. 3.

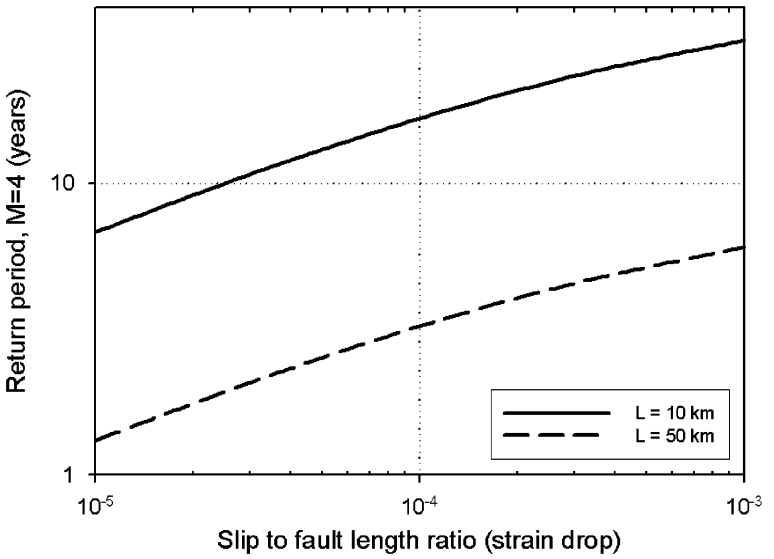

Fig. 6. Relation between return period for $M = 4$ earthquakes on a fault and the ratio between slip and fault length, for fault lengths of 10 and 50 km. Parameters otherwise are as for Fig. 3.

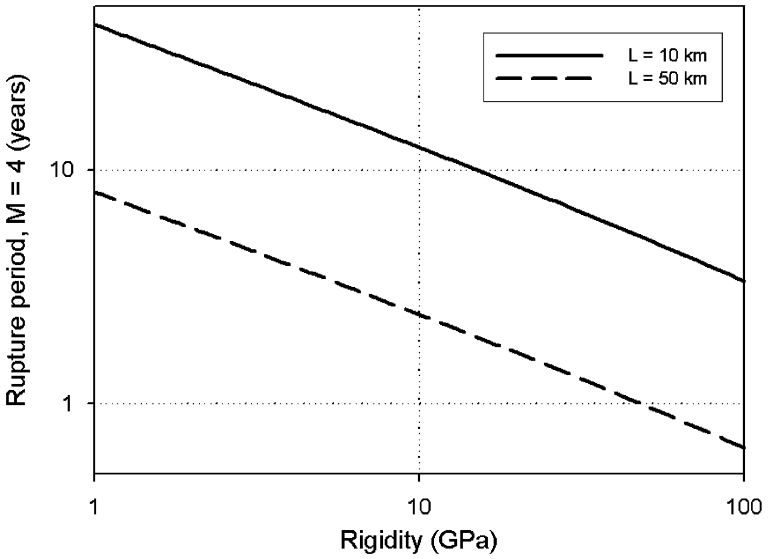

Fig. 7. Relation between return period for magnitude 4 earthquakes on a fault and the shear modulus, for fault lengths of 10 and 50 km. Parameters otherwise are as for Fig. 3.

3. Fault activity from seismic moment budgeting

In cases when direct slip rate estimates are not available, which is common even in plate margin regions, there might be other kinds of structural geological information available, supplemented by geodetic (such as GPS) observations, which could be used to infer, or at least to constrain, the slip rates and the associated geohazard potentials (e.g., Ward, 1994). If such approaches are not feasible one normally has to estimate, or at least to constrain, the seismic activity on the mapped faults from the regional seismicity, as deduced from historical and recent seismicity. This can be done, for example, by assigning a certain part (percentage) of the regional seismicity to the mapped faults, keeping the remaining for the area source(s) that receive their contributions from largely unmapped faults. This percentage can be applied directly to the N-values if the b-values are the same for area and fault sources,

Table 2
Input parameters used in the computer program "moment_rate", with examples of possible values

Line	Parameter	Example values		
1	Reference magnitude for N-value calculation	4.0		
2	Area zone N, b and M_{max}	1.0	1.0	7.0
3	Fault zone M_0-fraction, b-value and M_{max}	0.5	1.0	7.0
4	Moment–magnitude relation: $\log(M_0) = c + d \cdot M$	$c = 16.05$	$d = 1.50$	
5	Fault length (km), length/width factor	15.0	2.0	
6	Fault area to M_{max} relation: $\log(A) = a + b \cdot M_{max}$	$a = -4.15$	$b = 1.0$	
7	a-value step length; moment ratio convergence limit	0.01	0.001	
8	Maximum number of iterations; level of output details (0–2)	1000	2	

A fraction of 0.50 in line 3 means that 50% of the regional (area zone) seismicity is assumed to occur on the mapped fault for which activity rates will be estimated in this program. The algorithm works iteratively to determine the a-value that would produce a given moment rate, given a b-value.

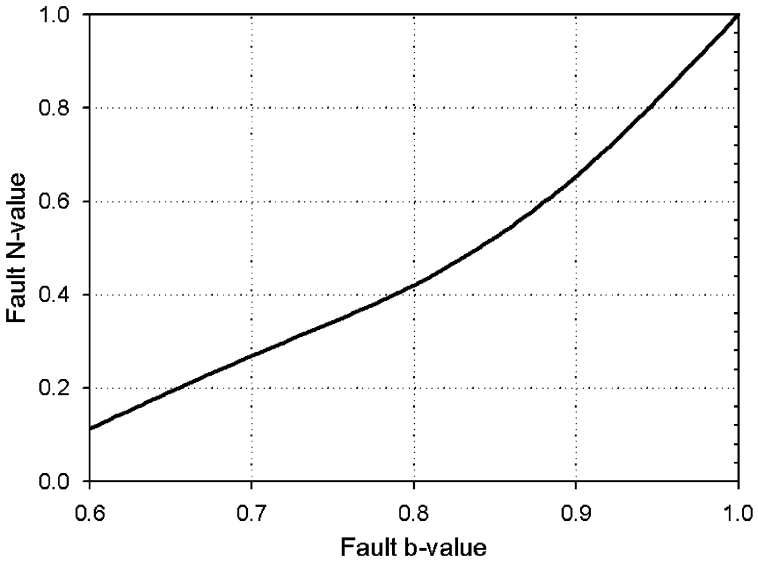

Fig. 8. Relation between N- and b-values on a fault, given the assumption that the fault always should capture all of the seismic moment that is released in the surrounding area zone, and with a maximum magnitude of 7. Parameters otherwise are as for Fig. 3.

but if the b-values are different the percentage has to be applied to the moment release, inferring a- or N-values indirectly. For this purpose another utility program ("moment_rate") has been developed, with a parameterization as seen in Table 2.

Essentially, this means that the fault is assumed to exhibit a certain moment rate, assessed in one way or the other, and based on a predefined b-value. The computer program then determines the a-value that would produce that moment rate, for a given functional form of the recurrence relation. The program works iteratively, based on integrating the seismic moment over the entire significant magnitude range.

Examples of how this computer program can be used are shown in the following. In Fig. 8 it is assumed that the area containing the fault has $N = 1$ events per year (above magnitude 4) and a b-value of 1.0, that all of the seismicity goes to the fault, and that the maximum magnitude for both the area and the fault is 7.0. The figure shows then the obvious result that the fault N-value will be 1.0 if the fault b-value is 1.0 as for the area, while for a b-value of 0.6 (which may not be an unrealistic value for faults) the corresponding N-value is almost down to 0.1. The obvious reason for this reduced a-value is that this is needed in order to keep the moment rate constant as the b-value decreases, thereby picking up more moment release near the maximum magnitude, in order to compensate for the reduction at lower magnitudes.

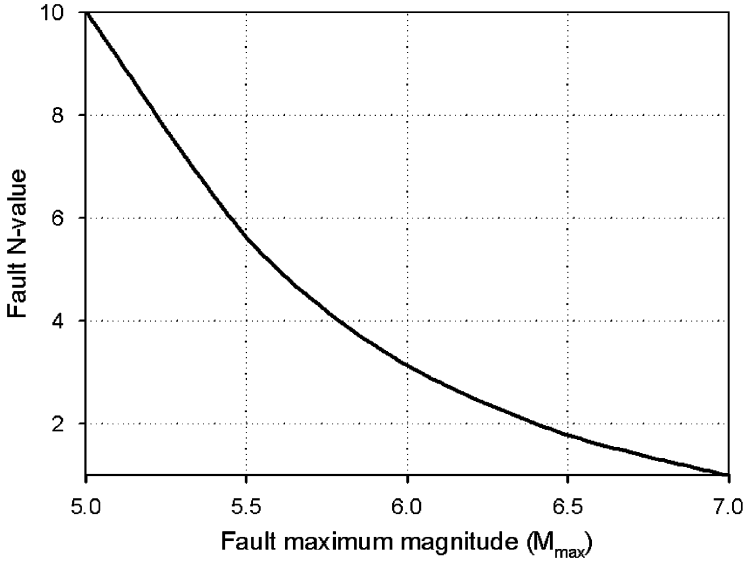

Fig. 9. Relation between N-values and maximum magnitude on a fault, given the assumption that the fault always should capture all of the seismic moment that is released in the surrounding area zone, and with a maximum magnitude of 7. Parameters otherwise are as for Fig. 3.

In the next example in Fig. 9 the fault N-value is shown as a function of maximum magnitude, the parameters otherwise being as for Fig. 8. When there is no difference in maximum magnitude ($M_{\max} = 7.0$) the N-value is of course 1.0, but as $M_{\max}$ decreases towards 5.0 the same moment rate release on the fault can be maintained only by increasing strongly the seismicity rate in terms of the N-value. This strong dependency on maximum magnitude results from the fact that most of the seismic moment comes from the highest magnitudes, even if the number of events there is lower. In principle this is well known, but it may be surprising to see how strong this effect is. This means that the moment release may be more sensitive to maximum magnitude than to the N-values, which for low exceedance probabilities may be important also in a seismic hazard context.

The ruling principle in all of this is that it is the seismic moment (or energy) budget which is the most important measure for expressing level of seismicity. Since many earthquake catalogues now use moment magnitude, this becomes easier to handle in a balanced way.

4. Selection of model parameters

The models presented above require the various parameters involved be determined in order for the activity rate represented by the N-value to be estimated (Anderson et al., 1993). These parameters are normally determined empirically, often dependent on the regional and local tectonic regimes. It is generally possible to estimate such parameters with less uncertainty in regions where deformation and seismicity rates are high, than in more stable regions such as most intraplate areas. Even there, however, maximum magnitudes may be high, they are just less frequent (Johnston and Kanter, 1990; Bungum et al., 2005). Plate margin areas certainly also pose major problems for the earthquake hazard analyst, basically in terms of epistemic uncertainties with respect to the seismic potentials, even of the more well-mapped faults. Naturally, the basic underlying problem is that any seismic hazard analysis is an exercise in predicting the future.

Some of the most important of these parameters are discussed briefly below, with emphasis on both plate margin and intraplate conditions, either in terms of commonly recommended values or as a range of possible values.

4.1. Moment–magnitude relationship

Numerous moment–magnitude relations are available for different regions and tectonic regimes, and for different types of magnitudes. Such regional relations may be used in cases when global relations (such as Okal and Romanowicz, 1993) or other regional relations (such as Ambraseys and Free,

1997, for Europe; see also Bungum et al., 2003) cannot be used. Such relations should be chosen with care, however, since the area-specific ones usually are based on poorer data, and therefore less reliable than the global ones. The main problem here is often that the larger magnitudes are missing, especially for intraplate regions, and it is recommended therefore to constrain such relations in the high-magnitude end by more stable global relations. Generally, however, the relation used should be applicable to the magnitudes that are used in the seismicity catalogues that the analysis is based on.

4.2. Fault slip to length ratio

This ratio is a proportionality constant between mean slip and fault length, where again plate margins are considerably better covered than intraplate areas. For such areas a value of 1.25×10^{-5} has earlier been suggested as a reasonable number, albeit conservative (Scholz, 1982). More recent results (Scholz et al., 1986; Scholz, 2002) have given support for values in the range $6–10 \times 10^{-5}$. Even more recently, however, results from the major postglacial faults in northern Fennoscandia have indicated values in excess of 10^{-4} (Muir Wood, 1993; Bungum et al., 2005), which clearly has significant implications for the near-field effects of large intraplate earthquakes.

4.3. Fault width to length ratio

The proportionality constant between the width W and the length L of the fault is another parameter that comes with large uncertainties, with large regional (tectonic) variations and a significant dependence on magnitude. The form of the ruptured area is often taken as being quadratic or rectangular, depending largely on earthquake size. A rectangular form, setting the width W equal to $\frac{2}{3}$ of the fault length L, may be a reasonable choice for larger intraplate events. For plate margin areas, however, the sensitivity to magnitude becomes more critical since larger earthquakes (say above $M = 6.7$) that reach the depth of the seismogenic (brittle) zone can grow only in the horizontal direction (Scholz, 2002). This is in turn related to the long discussion of whether slip scales with the length or the width of the fault (e.g., Scholz, 1994; Romanowicz, 1994; Wang and Ou, 1998).

4.4. Maximum magnitude

The maximum magnitude possible on a certain fault is also very difficult to assess, especially in regions of moderate and low seismicity where observational data from large magnitude earthquakes are scarce. In Fig. 2 we have shown a number of such relations, including a global relation by Wyss (1979) and an intraplate one by Nuttli (1983), the latter showing a very different slope. More recently, Wells and Coppersmith (1994) have provided a detailed analysis of empirical correlations between magnitude and fault dimensions, surface and subsurface, for different modes of faulting (see Fig. 2). As expected, these regressions show a considerable scatter around the mean. The way in which such relations change with magnitude also needs to be explored further.

In plate margin areas the maximum magnitude can in general be inferred from the length of the fault or a fault segment that is assumed to be able to rupture in one earthquake. This approach is, however, very uncertain, as demonstrated recently by the 1992 Landers (California) and the 1999 Denali (Alaska) earthquakes, both of which jumped between faults that were previously assumed to be unconnected. In spite of efforts to develop more sophisticated approaches for assessing maximum magnitude (Johnston, 1994), a useful practical rule is, like for activity rates, to base the assessment in part on the historical seismicity. A well-known rule-of-thumb here is to use a value for $M_{\max}$ 0.5 magnitude units above the largest one observed.

4.5. Rigidity modulus

The rigidity modulus is as already noted often set to a crustal average, in the lack of more detailed knowledge. For more shallow crustal conditions, however, and in particular for sedimentary rocks, the value may be significantly reduced, and with strong effects as already noted. In a study of subduction zone events, Bilek and Lay (1999) report values in the range between 1 GPa for near-surface conditions to more than 100 GPa at greater depths. The range of rigidity values for intraplate crystalline conditions will of course be much less than this, even though depth is important also here. This strong vertical variation in rigidity was the reason why Heaton and Heaton (1989) suggested the use of the potency (M_0/μ) as a more stable size-scaling

quantity, as also discussed by Anderson et al. (1993).

5. Concluding remarks

The computer programs documented in this paper require that the user specifies a range of models and model parameters that will influence the results, notably recurrence model (its functional form), slip rate, slip to length ratio, fault length and width, *b*-value, magnitude type, maximum magnitude (or fault area to maximum magnitude relation), moment–magnitude relation and shear modulus. It could have been useful to specify uncertainty ranges for all of these parameters in order to propagate these uncertainties to the top. When we have chosen not to do this, however, it has first of all been because this could easily be misleading as a way to model the overall uncertainties, since these also include, in fact are likely to be driven by, model uncertainties, in particular those relating to the basic recurrence relations. A recognized problem in this respect is the inadequacy of a short observational period as a basis for long-term estimates, as pointed out recently by Ambraseys (2006), who found that large earthquakes in many cases are less frequent when estimated from long-term data sets rather than from the instrumental period.

It is important to recognize these basic knowledge-based uncertainties that relate to inadequately understood geodynamic processes, in addition to the parametric uncertainties that may be improved with more and better data. In this sense it will be easy for a user of the present computer programs to replace the models and the relations, in order to accommodate for particular regional and data-specific requirements. The sensitivity tests that are an essential part of this paper besides presenting the models, are important since they will give the user an impression of the influence of each of the parameters, and also because some of the results are not necessarily intuitive. For example, in Figs. 3 and 4 the return period is seen to decrease with increasing fault length, which is because they all have the same slip rate and that a smaller maximum magnitude therefore will be compensated by a higher occurrence rate at lower magnitudes. We believe that such sensitivity tests are more useful to the user than what could be inferred from a specific test case taken from a model with only one specific fault length.

The two computer programs are small and simple utility programs of potential value first of all for the practising seismic hazard analyst. Earlier versions of the programs have been used by the author and his collaborators over many years, demonstrating the practical value. The programs are useful also as a tool for a detailed seismic moment budgeting when defining a source model for a seismic hazard study, where it is recommended to add the moment release from all of the sources (area zones and faults) in order to compare this not only with the regional historical seismicity but also with possible independent constraints, in particular geologic and geodetic information. Paleoseismological and other sources of long-term seismicity variations (e.g., Ambraseys, 2006) are important in this respect.

Acknowledgements

The author thanks Erik Hicks for assistance with some of the programming and Conrad D. Lindholm for detailed discussions and for advocating to make the computer programs available to the scientific community. The author also thanks Steven J. Gibbons and two anonymous reviewers for detailed comments that improved the paper considerably. ICG Contribution No. 35.

References

Aki, K., Richards, P.G., 2002. Quantitative Seismology, second ed. University Science Books, Sausalito, CA, 700pp.

Ambraseys, N.N., 2006. Comparison of frequency of occurrence of earthquakes with slip rates from long-term seismicity data: the cases of Gulf of Corinth, Sea of Marmara and Dead Sea Fault Zone. Geophysical Journal International 165, 516–526.

Ambraseys, N.N., Free, M.W., 1997. Surface-wave magnitude calibration for European region earthquakes. Journal of Earthquake Engineering 1, 1–22.

Anderson, J., 1979. Estimating the seismicity from geological structure for seismic-risk studies. Bulletin of the Seismological Society of America 69, 135–158.

Anderson, J.G., Luco, J.E., 1983. Consequences of slip rate constants on earthquake occurrence relations. Bulletin of the Seismological Society of America 73, 471–496.

Anderson, J.G., Ellis, M., Depolo, C., 1993. Earthquake rate analysis. Tectonophysics 218, 1–21.

Anderson, D.L., Wesnousky, S.G., Stirling, M.W., 1996. Earthquake size as a function of fault slip rate. Bulletin of the Seismological Society of America 86, 683–690.

Bakun, W.H., Aagaard, B., Dost, B., Ellsworth, W.L., Hardebeck, J.L., Harris, R.A., Ji, C., Johnston, M.J.S., Langbein, J., Lienkaemper, J.J., Michael, A.J., Murray, J.R., Nadeau, R.M., Reasenberg, P.A., Reichle, M.S., Roeloffs, E.A., Shakal, A., Simpson, R.W., Waldhauser, F., 2005. Implica-

tions for prediction and hazard assessment from the 2004 Parkfield earthquake. Nature 437, 969–974.

Båth, M., 1978. A note on recurrence relations for earthquakes. Tectonophysics 51, T23–T30.

Berril, J.B., Davis, R.O., 1980. Maximum entropy and the magnitude distribution. Bulletin of the Seismological Society of America 70, 1823–1831.

Bilek, S.L., Lay, T., 1999. Rigidity variations with depth along interplate megathrust faults in subduction zones. Nature 400, 443–446.

Bommer, J.J., Scherbaum, F., Bungum, H., Cotton, F., Sabetta, F., Abrahamson, N.A., 2005. On the use of logic trees for ground-motion prediction equations in seismic hazard analyses. Bulletin of the Seismological Society of America 95, 377–389.

Brune, J.N., 1968. Seismic moment, seismicity, and rate of slip along major fault zones. Journal of Geophysical Research 73, 777–784.

Bungum, H., Lindholm, C.D., Dahle, A., 2003. Long-period ground-motions for large European earthquakes, 1905–1992, and comparisons with stochastic predictions. Journal of Seismology 7, 377–396.

Bungum, H., Lindholm, C.D., Faleide, J.I., 2005. Postglacial seismicity offshore mid-Norway with emphasis on spatio-temporal-magnitudal variations. Marine and Petroleum Geology 22, 137–148.

Calais, E., Han, J.Y., DeMets, C., Nocquet, J.M., 2006. Deformation of the North American plate interior from a decade of continuous GPS measurements. Journal of Geophysical Research 111, B06402 doi: 10.1029/2005JB004253.

Chinnery, M.A., North, R.G., 1975. The frequency of very large earthquakes. Science 190, 1197–1198.

Coppersmith, K.J., Youngs, R.R., 1986. Capturing uncertainty in probabilistic seismic hazard assessments within intraplate tectonic environments. In: Proceedings of the Third U.S. National Conference on Earthquake Engineering, vol. 1, pp. 301–312.

Cornell, C.A., 1968. Engineering seismic risk analysis. Bulletin of the Seismological Society of America 58, 1583–1606.

Grant, L.B., 1996. Uncharacteristic earthquakes on the San Andreas Fault. Science 272, 826–827.

Hanks, T.C., Kanamori, H., 1979. A moment magnitude scale. Journal of Geophysical Research 84, 2348–2350.

Heaton, T.H., Heaton, R.E., 1989. Static deformations from point forces and force couples located in welded elastic Poissonian half spaces: implications for moment tensors. Bulletin of the Seismological Society of America 79, 813–841.

Johnston, A.C., 1994. Conclusions regarding maximum earthquake assessment. In: Johnston, A.C., Coppersmith, K.J., Kanter, L.R., Cornell, C.A. (Eds.), The earthquakes of stable continental regions. Technical Report EPRI TR-102261s-V1-V5, Electric Power Research Institute, Palo Alto, CA, 24pp.

Johnston, A.C., Kanter, L.R., 1990. Earthquakes in stable continental crust. Scientific American, 42–49.

Kanamori, H.D., Anderson, D.L., 1975. Theoretical basis for some empirical relations in seismology. Bulletin of the Seismological Society of America 65, 1073–1096.

Kulkarni, R.B., Youngs, R.R., Coppersmith, K.J., 1984. Assessment of confidence intervals for results of seismic hazard analysis. In: Proceedings of the Eighth World Conference on Earthquake Engineering, vol. 1. San Francisco, pp. 263–270.

Main, I.G., Burton, P.W., 1981. Rates of crustal deformation inferred from seismic moment and Gumbel's third distribution of extreme magnitude values. In: Beavers, J.E. (Ed.), Earthquakes and Earthquake Engineering: The Eastern United States, vol. 2, Ann Arbor Science, Ann Arbor, MI, Butterworth, London, pp. 937–951.

McGuire, R.K., 1976. FORTRAN computer program for seismic risk analysis. U.S. Geological Survey Open-File Report 76-67.

McGuire, R.K., 1978. FRISK: computer program for seismic risk analysis using faults as earthquake sources. U.S. Geological Survey Open-File Report 78-1007.

Molnar, P., 1979. Earthquake recurrence intervals and plate tectonics. Bulletin of the Seismological Society of America 69, 115–133.

Muir Wood, R., 1993. A review of the seismotectonics of Sweden. Report 43-01-R-001 for Svensk Kärnebränslehandtering AB (SKB), Stockholm, 225pp.

Nuttli, O.W., 1983. Average seismic source–parameter relations for mid-plate earthquakes. Bulletin of the Seismological Society of America 73, 519–535.

Okal, E.A., Romanowicz, B.A., 1993. On the variation of *b*-values with earthquake size. Physics of the Earth and Planetary Interiors 87, 55–76.

Papageorgiou, A.S., Aki, K., 1983. A specific barrier model for the quantitative description of inhomogeneous faulting and the prediction of strong ground motion. Bulletin of the Seismological Society of America 73, 693–722.

Romanowicz, B., 1994. Comment on "A reappraisal of large earthquake scaling" by C. Scholz. Bulletin of the Seismological Society of America 84, 1675–1676.

Scholz, C.H., 1982. Scaling laws for large earthquakes: consequences for physical models. Bulletin of the Seismological Society of America 68, 1–14.

Scholz, C.H., 1994. A reappraisal of large earthquake scaling. Bulletin of the Seismological Society of America 84, 215–218.

Scholz, C.H., 2002. The Mechanics of Earthquake Faulting, second ed. Cambridge University Press, Cambridge, 471pp.

Scholz, C.H., Aviles, C., Wesnousky, S., 1986. Scaling differences between large intraplate and interplate earthquakes. Bulletin of the Seismological Society of America 76, 65–70.

Swan III, F.H., Schwartz, D.P., Cluff, L.S., 1980. Recurrence of moderate-to-large magnitude earthquakes produced by surface faulting on the Wasatch fault zone. Bulletin of the Seismological Society of America 70, 1431–1462.

Wang, J.-H., Ou, S.-S., 1998. On scaling of earthquake faults. Bulletin of the Seismological Society of America 88, 758–766.

Ward, S.N., 1994. A multidisciplinary approach to seismic hazard in southern California. Bulletin of the Seismological Society of America 84, 1293–1309.

Wells, D.L., Coppersmith, K.J., 1994. New empirical relationships among magnitude, rupture length, rupture width, rupture area, and surface displacement. Bulletin of the Seismological Society of America 84, 974–1002.

Wyss, M., 1979. Estimating maximum expectable magnitude of earthquakes from fault dimensions. Geology 7, 336–340.

Yeats, R.S., Sieh, K., Allen, C.R., 1997. The Geology of Earthquakes. Oxford University Press, Oxford, 568pp.

Youngs, R.R., Coppersmith, K.J., 1985. Implications of fault slip rates and earthquake recurrence models to probabilistic seismic hazard estimates. Bulletin of the Seismological Society of America 75, 939–964.